

RESEARCH ARTICLE

Gradient-Informed Pareto-Based Multi-Objective Binary Topology Optimization

FRANCESCO LUCCHINI¹, RICCARDO TORCHIO^{1,2}, (Member, IEEE),
AND PIERGIORGIO ALOTTO¹

¹Department of Industrial Engineering, Università degli Studi di Padova, 35131 Padua, Italy

²Department of Information Engineering, Università degli Studi di Padova, 35131 Padua, Italy

Corresponding author: Francesco Lucchini (francesco.lucchini@unipd.it)

ABSTRACT Multi-objective topology optimization (TO) problems frequently arise in practical engineering applications, necessitating the identification of Pareto-optimal solutions. This article introduces a gradient-informed Pareto-based multi-objective TO algorithm with binary decision variables, called GPBTO, tailored to constrained bi-objective optimization problems (CBOPs), a common scenario in engineering design. By leveraging a binary decision space and incorporating a linearization step for objectives and constraints, the method enables the use of efficient integer linear programming (ILP) techniques for evolving the decision vector. Unlike traditional weighted sum (WS) approaches, which are widely used in TO despite their known limitations, GPBTO provides an alternative that integrates gradient-based formulations while facilitating the identification of Pareto-optimal solutions. While WS remains a dominant method in TO, GPBTO represents a promising alternative for cases where Pareto-based solutions are desirable. To the best of the authors' knowledge, this is the first attempt to integrate Pareto-based TO with binary variables and gradient information, highlighting its potential for further exploration and application.

INDEX TERMS Topology optimization (TO), large-scale multi-objective optimization, binary linear programming, gradient-search, Pareto-optimal solutions.

I. INTRODUCTION

In parallel with the advancements in additive manufacturing (AM) techniques, topology optimization (TO) has rapidly emerged as a cutting-edge methodology for tackling diverse engineering design hurdles, ranging from structural mechanics [1] to fluid dynamics [2], and electromagnetic applications [3], [4]. Being TO connected to a physical problem, the objective function f is derived from the numerical solution of a partial differential equation (PDE) in the design domain Ω_d , e.g., through a finite element analysis (FEA). Usually, TO is formulated as a constrained mono-objective optimization problem, written as:

$$\begin{aligned} \min \quad & f(\mathbf{u}(\mathbf{x}), \mathbf{x}) \\ \text{s.t.} \quad & \mathbf{x} \in \mathbb{S} \\ & g_i(\mathbf{x}) \leq 0, \quad i = 1, \dots, q, \end{aligned} \quad (1)$$

The associate editor coordinating the review of this manuscript and approving it for publication was Guolong Cui¹.

where \mathbf{x} is the array of decision variables defined in an appropriate space $\mathbb{S} \subset \mathbb{R}^n$, $g_i(\mathbf{x})$ is the i -th inequality constraint and q denotes the number of inequality constraints. In (1), the dependence of f with respect to \mathbf{u} , which is the solution of the FEA problem, is made explicit.

The decision variables are associated with each finite element discretizing Ω_d and they map the presence or absence of material with a certain property in such element. TO aims at finding the material distribution that minimizes a given objective under prescribed constraints. When the decision space \mathbb{S} is discrete (e.g., binary), each decision variable $x_i \in \{0, 1\}$. In this case, we refer to binary TO problems (also termed as ON/OFF [5]). The possibility of using binary decision variables for TO is very attractive to directly identify the void and filled parts in Ω_d as described subsequently.

Usually, (1) is solved with a gradient-based approach (gradient-based topology optimization or GTO). This is mainly due to historical reasons since TO was first studied in the context of structural mechanics, where the gradient of the usual

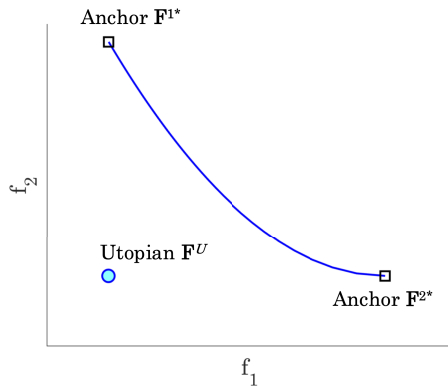


FIGURE 1. Illustrative example of PF for a BOP.

objective function can be easily evaluated. However, in the literature, alternative approaches are proposed to solve the TO task [6]. Beyond gradient-based methods, also evolutionary algorithms (EAs) are used with the remarkable advantage of avoiding the evaluation of the gradient of f [7]. Moreover, recently also neural-network (NN) based approaches have been proposed [8], [9]. EAs generally require the objective function to be evaluated many times for a given population \mathcal{P} , drastically increasing the CPU time for realistic problems for which f is obtained from the FEA solution of a PDE. A discussion concerning the usefulness of non-GTO (NGTO) methods is given in [10]. In particular [10]: “discusses the practical and scientific relevance of publishing papers that use immense computational resources for solving simple problems for which there already exist efficient solution techniques”. A notable exception of the NGTO algorithm, not based on traditional evolutionary strategies such as NSGA-II [11], is the proportional topology optimization (PTO) [12].

Performing TO for many practical engineering tasks [13], [14], requires the extension of constrained mono-objective optimization problems to constrained multi-objective optimization problems (CMOPs) written in the form:

$$\begin{aligned} \min \quad & \mathbf{F}(\mathbf{x}) = (f_1(\mathbf{x}), \dots, f_m(\mathbf{x})) \\ \text{s.t.} \quad & \mathbf{x} \in \mathbb{S} \\ & g_i(\mathbf{x}) \leq 0, \quad i = 1, \dots, q, \end{aligned} \quad (2)$$

where usually the dimension of the objective space $m = 2$, thus restricting to constrained bi-objective optimizations (CBOPs). CBOPs are very common in practical TO tasks [2], [15], [16]. When dealing with two conflicting objectives f_1, f_2 the CBOP solution must be understood in the Pareto sense. In the literature, CBOPs for TO accounting for the Pareto-optimal solutions, mainly through EAs, can be found [17], [18], [19], [20].

Historically CBOPs for TO are solved by using a gradient-based approach applied to the mono-objective function defined by combining f_1 and f_2 via a weighted sum (WS) approach [21], [22], [23], [24], [25]:

$$f = w_1 f_1 + w_2 f_2, \quad (3)$$

where w_1, w_2 are the weights, which can be adjusted during the algorithm iteration by exploiting, e.g., an adaptive weighted

sum (AWS) scheme [26], [27], [28], [29]. This method is valid as long as the Pareto front is convex, however, this statement cannot be verified in advance. Moreover, the selection of the weights is critical if f_1 and f_2 have different ranges of variation and dimensions, therefore a normalization step is required [26]. It is worth pointing out that, despite these limitations, WS approaches, thanks to their simple implementation strategies, represent the state-of-art methods for solving multi-objective TO problems, also combining more than two objectives [30], [31].

Gradient-based methods not based on the WS approach, such as the bi-descent algorithm, are also proposed in the literature [32], [33], [34]. This method can be used to construct general-shaped, e.g. non-convex, Pareto fronts, however, as outlined in [33], to construct the whole front, user-defined weight factors must be introduced.

Approaches combining gradient-based with EAs for multi-objective optimization have also been proposed [35], [36], [37].

To overcome the main limitations of the mentioned techniques, a gradient-informed Pareto-based CBOP for solving TO problems with binary decision variables is proposed. The algorithm is called GPBTO (gradient-informed Pareto-based binary TO). To the best of the author’s knowledge, this is the first attempt to solve Pareto-based TO using gradients and binary decision variables. The key contributions of the proposed algorithm are as follows:

- 1) *Population-based*: The proposed algorithm is population-based, i.e., many individuals are evolved during algorithm iterations in the same fashion as standard EAs, thus allowing parallelization.
- 2) *Gradient-informed evolution*: New individuals in the population are generated with a gradient-informed approach which is necessary for large-scale TO problems. The gradient-based approach avoids the generation of “bad” individuals reducing the number of objective functions evaluations.
- 3) *Integer linear programming*: The CBOP TO problem based on binary decision variables is linearized and the method of sequential linear integer programming (SLIP) is adopted. This opens up the possibility of using highly efficient ILP techniques to evolve the decision variables.
- 4) *Pareto-dominance*: The strategy of nondominated sorting and crowding distance (CD) is used to construct Pareto-optimal solutions.

The remainder of the article is organized as follows. Section II outlines the preliminaries and motivation of this work. The details of the proposed GPBTO are described in Section III. The performance of the algorithm is tested in Section IV. Conclusion are drawn in Section V.

II. PRELIMINARIES AND MOTIVATION

A. CONCEPTS OF PARETO DOMINANCE

A feasible decision vector \mathbf{x}_P it is said to *dominate* another decision vector \mathbf{x}_Q (written as $\mathbf{x}_P < \mathbf{x}_Q$) if $f_i(\mathbf{x}_P) \leq f_i(\mathbf{x}_Q)$

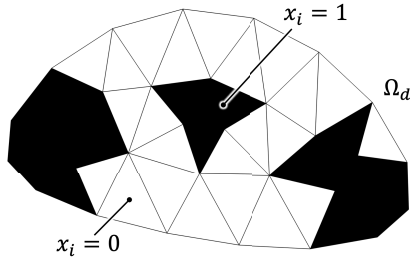


FIGURE 2. Illustrative example of binary decision variables for the TO problem within the design domain. The decision variable $x_i = 1$ if the material is present, $x_i = 0$ if the material is absent.

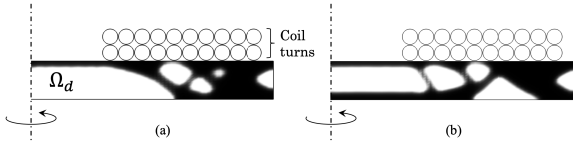


FIGURE 3. Final topology for the ferrite of an axisymmetric inductor within the framework of continuous TO starting from different decision vectors.

$\forall i = 1, \dots, m$ and exists at least one $j \in \{1, \dots, m\}$ for which $f_j(\mathbf{x}_P) < f_j(\mathbf{x}_Q)$. The set of all non-dominated decision vectors is called the Pareto set (PS) and the corresponding image in the objective function space is the Pareto front (PF).

Without loss of generality, for $m = 2$, defying with \mathbf{x}_1^* the solution of the single-objective minimization problem for f_1 , and with \mathbf{x}_2^* the solution of the single-objective minimization problem for f_2 , \mathbf{F}^U is the Utopian point in the f_1, f_2 plane defined as:

$$\mathbf{F}^U = (f_1(\mathbf{x}_1^*), f_2(\mathbf{x}_2^*)). \quad (4)$$

The i -th anchor point \mathbf{F}^{i*} is defined as:

$$\mathbf{F}^{i*} = (f_1(\mathbf{x}_i^*), f_2(\mathbf{x}_i^*)). \quad (5)$$

A sample graphical representation of a PF for a BOP is given in Fig. 1, where the Utopian, and anchor points are highlighted.

B. SETTING UP TOPOLOGY OPTIMIZATION

Mono-objective TO is the process that produces a material distribution inside a design domain Ω_d that minimizes an objective function under given constraints. Such objective function is derived from the solution of the PDE governing the physical problem in Ω_d . This task is one of the computational bottlenecks of the TO chain since the discretized form of the PDE, written as a system of equations:

$$\mathbf{K}(\mathbf{u}(\mathbf{x}), \mathbf{x})\mathbf{u}(\mathbf{x}) = \mathbf{b}(\mathbf{x}), \quad (6)$$

may require huge computational efforts for its solution, if the number of degrees of freedom (\mathbf{u}) is large, as common in many practical engineering problems. The matrix \mathbf{K} could be a function of both the array of unknowns \mathbf{u} (thus, resulting in a nonlinear problem) and the decision variables \mathbf{x} . Due to the physics-related nature of TO problems, no analytical benchmark objective functions can be used to test the performance of a TO algorithm as usually done with EAs,

Algorithm 1 Framework of ILP for Mono-Objective TO

```

1 Input:  $n, \beta, \epsilon, \bar{g}$ ;
2 Output:  $\mathbf{x}$ ;
3  $k \leftarrow 0$ ; /* iteration counter */
4  $\mathbf{x}^0 \leftarrow \text{Initialize}(n)$ ; /* initialize topology */
5 while termination criterion is not fulfilled do
6    $[f, dfdx] \leftarrow \text{EvaluateObjectiveAndGradient}(\mathbf{x}^k)$ ;
7    $[g, dgdx] \leftarrow \text{EvaluateConstraintAndGradient}(\mathbf{x}^k)$ ;
8    $\Delta \mathbf{x}^k \leftarrow \text{UpdateVariablesWithILP}(g, \bar{g}, dfdx, dgdx, \mathbf{x}^k)$ ;
9    $\mathbf{x}^{k+1} \leftarrow \mathbf{x}^k + \Delta \mathbf{x}^k$ ;
10   $k \leftarrow k + 1$ ;
11 end
12 return output

```

although some common test cases have become de-facto standards for performing comparisons [38].

When solving TO problems, the decision space is generally continuous, meaning that each decision variable assumes values in the interval as:

$$0 \leq x_i \leq 1, \forall i = 1, \dots, n \quad (7)$$

i.e., $\mathbb{S} = [0, 1]^n$. From the engineering viewpoint, the material property of the i -th finite element is not simply absent ($x_i = 0$) or present ($x_i = 1$), but may assume intermediate values corresponding to undetermined material specifications, also termed “gray scales”. These gray scales must be carefully addressed during the optimization steps by introducing the concepts of filtering and projection. The interested reader can find detailed information about these concepts in [39]. A clear distinction between filled and void regions, thus, avoiding gray scales, can be obtained by exploiting the concept of binary TO as illustrated in Fig. 2. In such a case the decision space $\mathbb{S} = \{0, 1\}^n$ is the product of binary sets and:

$$x_i \in \{0, 1\} \forall i = 1, \dots, n. \quad (8)$$

The usage of binary decision variables appears as a promising way for tackling the TO problem and in literature different algorithms based on this logic have been proposed, both with EAs and gradient-based approaches [40], [41], [42]. From a manufacturing perspective, using binary variables is advantageous as it clearly identifies the regions filled with material. However, the quality of the result depends on the number of mesh elements used for Ω_d . In contrast, using continuous variables allows for higher-order interpolation functions, providing greater flexibility.

It is worth noting that, being the number of decision variables equal to the number of finite elements discretizing Ω_d , TO falls into the class of large-scale optimization problems [43], [44], [45], [46]. This is why, generally, TO is solved with gradient-based methods, since a large number of decision variables may rapidly lead to the curse of dimensionality. It is well known that gradient-based approaches do not guarantee convergence to the global optimum and are sensitive to the initial guess \mathbf{x}^0 , as illustrated in Fig. 3. However, the result of a TO may be satisfactory once the constraints are fulfilled, even if the obtained topology is

a local optimum. In addition, a feasible solution is usually reached after a few algorithm iterations.

Many interpolation functions can be used to map the decision variable to the material property within the i -th finite element [47]. A simple scheme is given by the linear expression:

$$\mathcal{M}(x_i) = \mathcal{M}_{void} + (\mathcal{M}_{fill} - \mathcal{M}_{void}) x_i, \quad (9)$$

where \mathcal{M}_{void} is the value of the material property to be assigned to void elements ($x_i = 0$), while \mathcal{M}_{fill} is the value of the material property to be assigned when $x_i = 1$.

Being TO aimed at modifying the material distribution in Ω_d , a natural constraint is imposed in the final amount of material (e.g., with $x_i = 1$). This corresponds to a volumetric constraint, usually written in terms of an inequality constraint:

$$V(\mathbf{x}) = \sum_i v_i x_i \leq \bar{V} V_{\Omega_d} \quad (10)$$

where v_i is the volume of i -th finite element, \bar{V} is the volume fraction ($0 \leq \bar{V} \leq 1$), and V_{Ω_d} is the volume of the whole Ω_d .

From Fig. 3 it can be argued one of the major limitations of the continuous TO approach, i.e., the blurring of the boundary regions between $x = 1$ and $x = 0$. In particular, from a manufacturing point of view, the boundary must be precisely defined, and the cutting procedure may introduce variations in the results. Using binary variables not only has the advantage of easily distinguishing the region occupied by the material compared to the empty spaces but also has repercussions on the type of algorithms that can be used to solve the optimization problem, as described in Section II-D. In the remainder of this work, the binary TO approach is used.

C. EVALUATION OF GRADIENTS

The gradients of objectives and constraints are required to advance the design variables within the framework of TO. This represents the main bottleneck of gradient-based optimization methods from the computational viewpoint. For example, considering a function $f(\mathbf{x})$, the algorithm requires the evaluation of the ‘‘sensitivity’’ defined as the array:

$$\mathbf{S}(\mathbf{x}) = \left(\frac{df(\mathbf{x})}{dx_1}, \dots, \frac{df(\mathbf{x})}{dx_n} \right). \quad (11)$$

In the literature, different approaches have been used to this aim, mainly based on the adjoint variable method (AVM) [48], which is very attractive for self-adjoint objective functions as is usually the case in structural mechanics TO problems. It is worth mentioning that automatic differentiation techniques have been recently applied [49]. It is important to note that the gradient of the volumetric constraint (10) is trivial and corresponds to the array collecting the volumes of finite elements \mathbf{v} .

D. MONO-OBJECTIVE TOPOLOGY OPTIMIZATION WITH ILP

ILP has been conveniently applied to solve constrained mono-objective TO problems with binary decision variables in [42], [50], [51], [52], and [53]. A detailed description of

Algorithm 2 Framework of Proposed Algorithm

```

1 Input:  $n, N, \beta_{min}, \epsilon, \bar{g}, k_{max}$ ;
2 Output:  $\mathcal{P}$ ;
3  $k \leftarrow 0$ ; /* iteration counter */
4  $\mathcal{F}_1 \leftarrow \emptyset$ ;
5  $\mathcal{F}_2 \leftarrow \emptyset$ ;
6  $\mathcal{G} \leftarrow \emptyset$ ;
7  $d\mathcal{F}_1 \leftarrow \emptyset$ ;
8  $d\mathcal{F}_2 \leftarrow \emptyset$ ;
9  $d\mathcal{G} \leftarrow \emptyset$ ;
10  $\mathcal{P}^0 \leftarrow Initialize(n, N)$ ; /* random initialization */
11  $\mathcal{P}^0 \leftarrow Blurring(\mathcal{P}^0)$ ;
12 for  $\mathbf{x} \in \mathcal{P}^0$  do
13   evaluate objectives, constraint, and derivatives;
14    $\mathcal{F}_1 \leftarrow \mathcal{F}_1 \cup f_1$ ;
15    $\mathcal{F}_2 \leftarrow \mathcal{F}_2 \cup f_2$ ;
16    $\mathcal{G} \leftarrow \mathcal{G} \cup g$ ;
17    $d\mathcal{F}_1 \leftarrow d\mathcal{F}_1 \cup df_1 dx$ ;
18    $d\mathcal{F}_2 \leftarrow d\mathcal{F}_2 \cup df_2 dx$ ;
19    $d\mathcal{G} \leftarrow d\mathcal{G} \cup dg dx$ ;
20 end
21  $\mathcal{A} \leftarrow \emptyset$ ; /* initialize archive */
22 put  $\mathcal{P}^0, \mathcal{F}_1, \mathcal{F}_2, \mathcal{G}, d\mathcal{F}_1, d\mathcal{F}_2$ , and  $d\mathcal{G}$  into the archive  $\mathcal{A}$ ;
23  $I \leftarrow \emptyset$ ;
24 while termination criterion is not fulfilled do
25   get current size of  $\mathcal{A}$ :  $S(\mathcal{A})$ ;
26    $\mathcal{F}_1 \leftarrow \emptyset$ ;
27    $\mathcal{F}_2 \leftarrow \emptyset$ ;
28    $\mathcal{G} \leftarrow \emptyset$ ;
29    $d\mathcal{F}_1 \leftarrow \emptyset$ ;
30    $d\mathcal{F}_2 \leftarrow \emptyset$ ;
31    $d\mathcal{G} \leftarrow \emptyset$ ;
32    $\beta \leftarrow UpdateBeta(\beta_{min}, k, k_{max})$ ; /* update  $\beta$  */
33   if  $S(\mathcal{A})$  greater than  $N/2$  then
34     construct  $I_1$  with indices from 1 to  $N/2$ ;
35     construct  $I_2$  with  $N/2$  random indices from  $N/2$  to  $S(\mathcal{A})$ ;
36      $I \leftarrow I_1 \cup I_2$ ;
37   else
38     construct  $I$  with  $N/2$  random indices from 1 to  $S(\mathcal{A})$ ;
39   end
40   for  $l \in I$  do
41     select  $l$ -th individual  $\mathbf{x}$  from  $\mathcal{A}$  together with its values of  $f_1$ ,
42      $f_2, g, df_1 dx, df_2 dx, dg dx$ ;
43     compute new individual  $\hat{\mathbf{x}}$  with ILP following  $df_1 dx$ ;
44     put  $\hat{\mathbf{x}}$  into  $\mathcal{P}$ ;
45      $[f_1^{\hat{\mathbf{x}}}, df_1 d\hat{\mathbf{x}}] \leftarrow EvaluateObjectiveAndGradient(\hat{\mathbf{x}})$ ;
46      $[f_2^{\hat{\mathbf{x}}}, df_2 d\hat{\mathbf{x}}] \leftarrow EvaluateObjectiveAndGradient(\hat{\mathbf{x}})$ ;
47      $[g^{\hat{\mathbf{x}}}, dg d\hat{\mathbf{x}}] \leftarrow EvaluateConstraintAndGradient(\hat{\mathbf{x}})$ ;
48     store  $f_1^{\hat{\mathbf{x}}}, f_2^{\hat{\mathbf{x}}}$  into  $\mathcal{F}_1, \mathcal{F}_2$ ;
49     store  $g^{\hat{\mathbf{x}}}$  into  $\mathcal{G}$ ;
50     store  $df_1 d\hat{\mathbf{x}}, df_2 d\hat{\mathbf{x}}$  into  $d\mathcal{F}_1, d\mathcal{F}_2$ ;
51     store  $dg d\hat{\mathbf{x}}$  into  $d\mathcal{G}$ ;
52     compute new individual  $\tilde{\mathbf{x}}$  with ILP following  $df_2 dx$ ;
53     store  $\tilde{\mathbf{x}}$  into  $\mathcal{P}$ ;
54      $[f_1^{\tilde{\mathbf{x}}}, df_1 d\tilde{\mathbf{x}}] \leftarrow EvaluateObjectiveAndGradient(\tilde{\mathbf{x}})$ ;
55      $[f_2^{\tilde{\mathbf{x}}}, df_2 d\tilde{\mathbf{x}}] \leftarrow EvaluateObjectiveAndGradient(\tilde{\mathbf{x}})$ ;
56      $[g^{\tilde{\mathbf{x}}}, dg d\tilde{\mathbf{x}}] \leftarrow EvaluateConstraintAndGradient(\tilde{\mathbf{x}})$ ;
57     store  $f_1^{\tilde{\mathbf{x}}}, f_2^{\tilde{\mathbf{x}}}$  into  $\mathcal{F}_1, \mathcal{F}_2$ ;
58     store  $g^{\tilde{\mathbf{x}}}$  into  $\mathcal{G}$ ;
59     store  $df_1 d\tilde{\mathbf{x}}, df_2 d\tilde{\mathbf{x}}$  into  $d\mathcal{F}_1, d\mathcal{F}_2$ ;
60     store  $dg d\tilde{\mathbf{x}}$  into  $d\mathcal{G}$ ;
61   end
62   put  $\mathcal{P}, \mathcal{F}_1, \mathcal{F}_2, \mathcal{G}, d\mathcal{F}_1, d\mathcal{F}_2$ , and  $d\mathcal{G}$  into the archive  $\mathcal{A}$ ;
63    $k \leftarrow k + 1$ ;
64 end
65 return output

```

such an approach is out of the scope of this paper, however, in what follows the basic principles are outlined. The idea is

based on a linearization procedure (of objective and constraint functions) of the TO problem (1) around a given array of decision variables \mathbf{x}^k , where k is the iteration counter, in the form:

$$f(\mathbf{x}) \approx f(\mathbf{x}^k) + \left. \frac{df(\mathbf{x})}{d\mathbf{x}} \right|_{\mathbf{x}=\mathbf{x}^k} \cdot (\mathbf{x} - \mathbf{x}^k). \quad (12)$$

Following [42] and restricting the analysis to a single constraint ($q = 1$), the TO problem is transformed into the following SLIP:

$$\begin{aligned} \min \quad & \frac{df(\mathbf{x}^k)}{d\mathbf{x}} \cdot \Delta\mathbf{x}^k \\ \text{s.t.} \quad & \frac{dg(\mathbf{x}^k)}{d\mathbf{x}} \cdot \Delta\mathbf{x}^k \leq \Delta g(\mathbf{x}^k) \\ & \|\Delta\mathbf{x}^k\|_1 \leq \beta n \\ & \Delta x_j^k \in \{-x_j^k, 1 - x_j^k\} \quad j \in \{1, \dots, n\}, \end{aligned} \quad (13)$$

where:

$$\Delta g(\mathbf{x}^k) = \begin{cases} -\epsilon g(\mathbf{x}^k) : \bar{g} < (1 - \epsilon)g(\mathbf{x}^k) \\ \bar{g} - g(\mathbf{x}^k) : \bar{g} \in [(1 - \epsilon)g(\mathbf{x}^k), (1 + \epsilon)g(\mathbf{x}^k)] \\ \epsilon g(\mathbf{x}^k) : \bar{g} > (1 + \epsilon)g(\mathbf{x}^k). \end{cases} \quad (14)$$

The decision vector at iteration $k + 1$ is given by $\mathbf{x}^{k+1} = \mathbf{x}^k + \Delta\mathbf{x}^k$. It is worth noting that two user-controlled parameters appear in (13) and (14), i.e. β and ϵ . These two quantities represent the fraction of decision variables that can change between two consecutive iterations (flip limits) and a constraint relaxation parameter. The effect of their variation on the final topology in the context of multi-objective TO problems is investigated in Section IV-B.

The SLIP (13) can be solved with ILP, for example using IBM ILOG CPLEX Optimization Studio, the *intlinprog* function of MATLAB[®], or other approaches mentioned in, e.g., [54]. A schematic framework of ILP for solving TO problems with binary variables is listed in Algorithm 1.

III. PROPOSED ALGORITHM

In this section, the GPBTO algorithm is described. Only the implementation steps for the bi-objective TO with a single constraint are listed in Algorithm 2, however, as described later, the extension to m objectives is straightforward. It is worth recalling that CBOPs are very common in TO problems, thus the proposed algorithm can already be used to solve real engineering problems. In what follows, an insight into the most important steps highlighted in Algorithm 2 is given. Particularly, the salient steps are highlighted with different colors.

The construction of the initial population is described in Section III-A and the management of the archive to obtain Pareto-optimal solutions is explained in Section III-B. A strategy for updating β during algorithm iterations is proposed in Section III-C. The objective, constraint, and gradient evaluations are explained in Section III-D, while

Algorithm 3 Blurring

```

1 Input:  $\mathbf{x}^0, \mathbf{v}, \bar{V}, V_{\Omega_d}$ ;
2 Output:  $\mathbf{x}_b$ ;
3  $\tilde{\mathbf{x}} \leftarrow \text{Filtering}(\mathbf{x}^0)$ ; /* filtering via Eq. (15) */
4  $idx \leftarrow \text{Sorting}(\tilde{\mathbf{x}})$ ; /* sort  $\tilde{\mathbf{x}}$  in descending order and
   get the index map of transformation */
5  $k \leftarrow 1$ ;
6  $I \leftarrow \emptyset$ ;
7  $V \leftarrow 0$ ;
8 while  $V \leq \bar{V} V_{\Omega_d}$  do
9    $I \leftarrow I \cup idx(k)$ ; /* Update index set */
10   $V \leftarrow V + \mathbf{v}(k)$ ; /* Update volume */
11   $k \leftarrow k + 1$ ;
12 end
13  $\mathbf{x}_b \leftarrow \mathbf{0}$ ; /* Initialize output decision vector */
14  $\mathbf{x}_b(I) \leftarrow \mathbf{1}$ ; /* Fill the output decision vector with
   ones in positions  $I$  */
15 return output

```

the update of the decision vector through ILP is described in Section III-E.

A. INITIAL POPULATION GENERATION

Being the TO strictly related to the physical problem, the construction of the initial configuration must be carefully addressed. Within the GPBTO framework, the initialization is performed in line 10 of the Algorithm 2, where k is the iteration counter. In the framework of mono-objective TO, very often the whole Ω_d is filled with material, thus, $x_i = 1 \forall i = 1, \dots, n$. The proposed algorithm is a population-based one, with an initial population \mathcal{P}^0 of N randomly generated configurations. However, the topologies obtained in this way are likely to be formed by many disconnected clusters giving rise to checkerboard patterns [55]. Following [56], a blurring technique is used in the proposed algorithm to adjust the initial population, satisfying the volumetric constraint defined by (10). This procedure is applied to \mathcal{P}^0 at line 11 of the Algorithm 2. Starting from \mathcal{P}^0 the blurring technique for $\mathbf{x} \in \mathcal{P}^0$ is based on two steps:

- 1) Filtering of the decision variables: as shown in Fig. 4(b), this step assigns to each decision variable a continuous value obtained as the mean of neighborhood values [39]:

$$\tilde{x}_i = \frac{\sum_{j \in \mathbb{N}(i)} w(\mathbf{r}_j) v_j x_j}{\sum_{j \in \mathbb{N}(i)} w(\mathbf{r}_j) v_j}, \quad (15)$$

thus resulting in a blurred topology. In (15), $\mathbb{N}(i)$ is the neighborhood set of mesh elements lying within the filter domain for element i and $w(\mathbf{r}_j)$ is a weighting function of each barycenter coordinate \mathbf{r}_j of j -th mesh element [39].

- 2) Definition of clusters satisfying the volumetric constraint: next, the decision variables with higher values in $[0, 1]$ are selected until the volume constraint is satisfied (10). The output of this step is illustrated in Fig. 4(c).

It is worth noting that the blurring technique does not guarantee connectivity between clusters but helps generate an initial

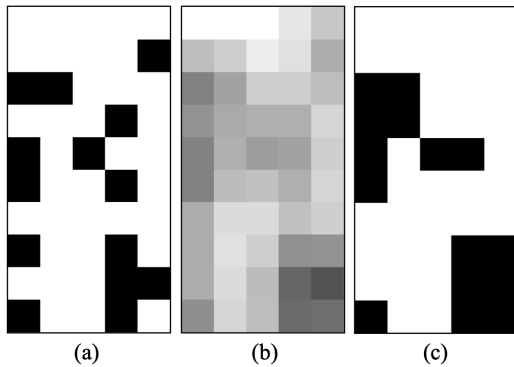


FIGURE 4. Blurring technique. Initial topology (a). Filtering (b). Generation of clusters (c).

population with few clusters with small dimensions. To enrich the quality of the first population, some individuals are computed as solutions of the scalarized BOP. In particular, the two anchor points highlighted in Fig. 1 are included in the initial population.

The objective functions, the constraints, and the related derivatives are evaluated for each member of the population, the results are stored in \mathcal{F}_1 , \mathcal{F}_2 , \mathcal{G} , $d\mathcal{F}_1$, $d\mathcal{F}_2$, and $d\mathcal{G}$.

B. ARCHIVE MANAGEMENT

The archive \mathcal{A} collects the population \mathcal{P} (up to a prescribed dimension $N_{\mathcal{A}}$) together with the values of f_1 , f_2 , g , $df_1/d\mathbf{x}$, $df_2/d\mathbf{x}$, and $dg/d\mathbf{x}$ for each individual $\mathbf{x} \in \mathcal{P}$. GPBTO uses the archive to memorize the mentioned quantities in lines 22 and 61 of the Algorithm 2. As an example, \mathcal{F}_1 stores f_1 values, while \mathcal{F}_2 stores f_2 values. To move towards the Pareto-optimal solutions, the nondominated sorting and CD techniques [11] are used in the proposed algorithm. The former technique subdivides the population in \mathcal{A} into several fronts with different ranks (with rank-1 higher than rank-2, rank-3, and so on) exploiting the concept of Pareto dominance described in Section II-A. The CD is used to construct well-resolved PFs. Low-rank individuals or individuals with high CD, when their rank is the same, are preferred. A detailed description of the mentioned approach for generating Pareto-optimal solutions is out of the scope of the paper, however, the interested reader can find more information in [57].

1) CONSTRAINT HANDLING

Many approaches have been proposed in the literature to manage the constraints in CMOPs [58], [59]. In the proposed algorithm the constraint domination principle (CDP), described in [60], is used within the archive management procedure to incrementally favor feasible solutions over infeasible ones, i.e.:

- If a solution \mathbf{x}_1 is feasible and \mathbf{x}_2 is unfeasible, \mathbf{x}_1 is ranked above \mathbf{x}_2 .
- If both \mathbf{x}_1 and \mathbf{x}_2 are feasible the Pareto dominance concept (see Section II-A) is used to rank the two solutions.
- If the two solutions are both unfeasible, the one with smaller constraints violation is ranked higher.

C. UPDATING β PARAMETER

A strategy for updating β during the iterations is proposed since it seems not convenient to use a constant value of β to control the change of design variables [50], [52]. In the proposed algorithm, on line 32, the following rule is adopted:

$$\beta(k) = \beta_{min} + (\beta_{max} - \beta_{min}) \frac{(k_{max} - k)^\gamma}{(k_{max} - 1)^\gamma}, \quad (16)$$

where k is the iteration counter, k_{max} the maximum number of iterations, β_{min} the minimum value of β , β_{max} the maximum value, and $\gamma > 1$ an exponent. In this way, at the beginning of iterations, the algorithm is more explorative (a large fraction of decision variables may change), becoming more exploitative (a small fraction of decision variables is allowed to change status) when the algorithm proceeds. The effect of β variation during the algorithm iterations is examined in the numerical experiments section.

D. EVALUATION OF OBJECTIVE, CONSTRAINT, AND GRADIENT

The evaluation of objective, constraint, and gradient values, which are problem-dependent, is performed within the GPBTO framework in lines 13, 44–46, and 53–55 of Algorithm 2, for the case of bi-objective problems. There, given an individual of the population, the objective function is extracted from the solution of the PDE governing the physics, together with the value of constraints and gradients, following the discussion of Section II-C.

E. UPDATING DECISION VECTOR WITH ILP

A new individual of the population is computed by solving the ILP similarly to the mono-objective TO problem. This step is performed in lines 42 and 51 of the Algorithm 2. Within the proposed algorithm an additional constraint is added to the value of the objective function which is not considered in the minimization step. For example, once using $df_1/d\mathbf{x}$ to get the new individual $\hat{\mathbf{x}}$ from \mathbf{x} , the value of f_2 is constrained in such a way that:

$$f_2(\mathbf{x}) \leq \bar{f}_2(\mathbf{x}) = f_2(\mathbf{x}) + \alpha |f_2(\mathbf{x})| \quad (17)$$

for some $\alpha > 0$. After the linearization step, as in (13), this additional constraint is added to ILP. By doing this the optimizer is free to worsen f_2 while optimizing f_1 , fixing an upper bound for the worsening. The same concept is applied when f_2 is optimized. To extend the algorithm to $m > 2$ objectives, the updating procedure must be adjusted. This is theoretically straightforward, as the function used to solve the ILP (e.g., *intlinprog*) can handle multiple constraints. Specifically, while optimizing f_i , a vector of constraints of the form (17) must be imposed for f_j ($i \neq j$). However, numerical tests would be necessary to fully validate the effectiveness of this extension.

F. COMPUTATIONAL COMPLEXITY

The computational complexity of GPBTO depends on objectives, constraints, gradient evaluations, ILP, and archive

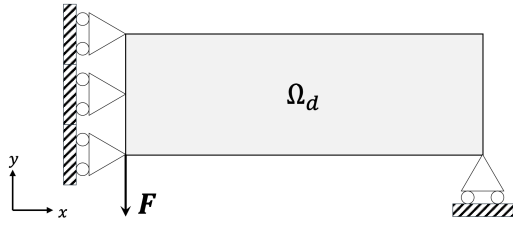


FIGURE 5. Domain and boundary conditions for the MBB beam.

management. For a population of N individuals each of size n , the time complexity for objective, constraints, and gradients is $\mathcal{O}(N)$. The ILP used to update the binary decision vector based on the branch-and-bound algorithm has a worst-case theoretical time complexity of $\mathcal{O}(2^n)$. It is worth mentioning that this is the worst-case, however, for practical optimization problems the complexity is much less [61]. For m objective functions ($m = 2$ in the proposed GPBTO), the nondominated sorting plus CD used for archive management have a time complexity of $\mathcal{O}(mN^2)$ and $\mathcal{O}(mN \log N)$ [111].

G. PARALLELIZATION

The GPBTO algorithm can be trivially parallelized since the construction of new individuals from the l -th one within \mathcal{A} is independent of the other individuals with index $i \neq l$.

IV. NUMERICAL EXPERIMENTS

In this section, the GPBTO algorithm is used to solve CBOPs of classical structural mechanics benchmarks. A performance indicator is introduced in Section IV-A. The performances of the proposed algorithm as a function of user-defined parameters are evaluated in the example reported in Section IV-B. In Section IV-B, the GPBTO is used for the design of a compliant mechanism, a well-known CBOP problem in TO.

A. PERFORMANCE INDICATOR

The inverted geometrical distance (IGD), representing the averaged distance from each reference point to its nearest solution, is commonly adopted as a performance indicator [62]. It is worth pointing out that, since the standard IGD is Pareto non-compliant, different metrics have been proposed as performance indicators. In this paper, the modified inverted geometrical distance (IGD⁺) described in [63] is used. Given a solution set A , with cardinality $|A|$, and a reference set Z of cardinality $|Z|$, the IGD⁺ is computed as [63]:

$$IGD^+(A) = \frac{1}{|Z|} \sum_{k=1}^{|Z|} d^+(z_k, \mathbf{a}_{j(k)}), \tag{18}$$

where $d^+(\cdot, \cdot)$ is the modified distance calculation which for minimization problems is expressed as:

$$d^+(z, \mathbf{a}) = \sqrt{\sum_{i=1}^m (\max\{a_i - z_i, 0\})^2}, \tag{19}$$

where m is again the dimension of the objective space as defined in (2). In (18), $\mathbf{a}_{j(k)}$ with $j(k) \in \{1, \dots, |A|\}$, is the

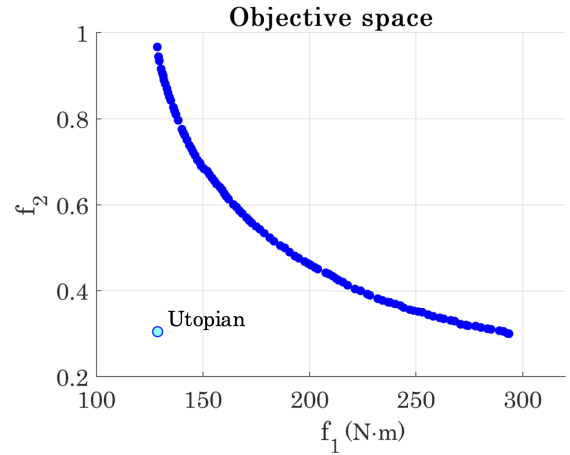


FIGURE 6. PF of BOP TO problem for MBB beam.

nearest objective array to the point z_k . Smaller values of IGD⁺ mean better performances.

B. PARAMETER SETTINGS

The performance of the proposed algorithm against the user-defined parameters is tested in this example. The Messerschmitt-Bölkow-Blohm (MBB) beam, whose domain and boundary conditions are illustrated in Fig. 5, is a classical example to test the performance of mono-objective TO algorithms and is selected as a benchmark. Physically, the linear elasticity problem described by the PDE:

$$\nabla \cdot \mathbf{S} + \mathbf{F} = 0, \tag{20}$$

where \mathbf{S} is the Piola stress and \mathbf{F} is the body force, is solved in Ω_d by using a FEA approach resulting in the system of equations $\mathbf{K}\mathbf{u} = \mathbf{f}$, where \mathbf{K} is the stiffness matrix. A detailed description of the steps of the FEA analysis can be found e.g., in [64]. In this example, a uniform grid consisting of $n_x = 120$ elements along x -coordinate and $n_y = 40$ elements along y -coordinate is used to discretize Ω_d , resulting in $n = 4800$ decision variables.

The purpose of the TO is to find out the distribution of the material by modifying the value of Young’s modulus E within each mesh element through (9), where $\mathcal{M}_{void} = E_{void} = 10^{-4}$ Pa and $\mathcal{M}_{fill} = E_{fill} = 1$ Pa. Being the stiffness matrix function of the material properties within the computational domain, \mathbf{K} is a function of the decision vector, which changes during the optimization steps, i.e., $\mathbf{K} = \mathbf{K}(\mathbf{x})$. Thus, also the solution array \mathbf{u} is a function of the current distribution of \mathbf{x} , while the load vector \mathbf{f} is constant.

Many research papers proposed a bi-objective TO to minimize the following objective functions:

$$\begin{aligned} f_1(\mathbf{x}) &= \mathbf{u}^T(\mathbf{x})\mathbf{K}(\mathbf{x})\mathbf{u}(\mathbf{x}) \\ f_2(\mathbf{x}) &= V(\mathbf{x})/V_{\Omega_d} \end{aligned} \tag{21}$$

respectively corresponding to the strain energy (SE) and the material volume defined in (10). However, the multi-objective extension is only performed in the WS sense [22]. The PF

TABLE 1. Effect of flip limits (β).

β	ϵ	N	k_{max}	Best	Worst	Ave.	Std.
0.5	0.01	20	100	14.8E-3	45.4E-3	22.9E-3	7.1E-3
0.1	0.01	20	100	13.6E-3	38.2E-3	24.2E-3	6.9E-3
0.01	0.01	20	100	6.1E-3	128.1E-3	23.5E-3	31.1E-3
0.005	0.01	20	100	65.1E-3	258.4E-3	165.1E-3	59.5E-3
0.5 \rightarrow 0.005	0.01	20	100	6.5E-3	23.5E-3	11.2E-3	5E-3

TABLE 2. Effect of constraint relaxation (ϵ).

ϵ	N	k_{max}	Best	Worst	Ave.	Std.
0.1	20	100	11E-3	68.7E-3	24.5E-3	14.7E-3
0.05	20	100	14.8E-3	117.5E-3	30.2E-3	23.4E-3
0.02	20	100	6.1E-3	28E-3	15.9E-3	6.4E-3
0.01	20	100	6.5E-3	23.5E-3	11.2E-3	5E-3
0.005	20	100	3.8E-3	13E-3	7.2E-3	2.1E-3
0.001	20	100	6.1E-3	28.4E-3	12.4E-3	6E-3

 β : 0.5 \rightarrow 0.005**TABLE 3.** Effect of population size.

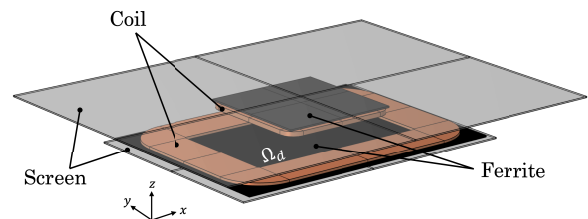
N	k_{max}	Tot.	Best	Worst	Ave.	Std.
50	40	2000	4.8E-3	19.4E-3	8.9E-3	3.6E-3
40	50	2000	5.2E-3	19.7E-3	10.9E-3	4.1E-3
20	100	2000	3.8E-3	13E-3	7.2E-3	2.1E-3
10	200	2000	5.3E-3	21E-3	9.2E-3	4.8E-3
8	250	2000	5.5E-3	65E-3	17.7E-3	13.9E-3

 β : 0.5 \rightarrow 0.005
 $\epsilon = 0.005$

obtained with the GPBTO algorithm is illustrated in Fig. 6. The resulting PF is convex, thus, the applicability of the WS approach is justified for this particular case. In what follows, the performance of the proposed algorithm under the variation of the user-defined parameters, namely β , ϵ , N , and k_{max} is verified. In particular, the IGD^+ values are computed over 20 independent runs, and the best, worst, mean (Ave.), and standard deviation (Std.) values are collected. All the tests are performed by keeping the product $N \cdot k_{max}$ constant, corresponding to the maximum number of objective function evaluations. The maximum dimension of the archive N_A is set to 100.

The effect of β variation is listed in Table 1. The best performances in terms of IGD^+ indicator, highlighted in the Table, are obtained when β is linearly changed from 0.5 to 0.005 during algorithm iterations (0.5 \rightarrow 0.005). This behavior is similar to the modified particle swarm optimizer (PSO) [65], for which better performances are achieved when the weight of the inertial component is progressively reduced during algorithm iterations, to make the knowledge gained by the population increasingly more relevant.

It is worth pointing out that ϵ is fixed to 0.01 in this case. This value is retrieved from [42] and represents a good compromise. Adopting a linear variation strategy for β , the effect of the ϵ parameter on the algorithm performances is tested. In this case, better performances, highlighted in Table 2, are obtained for low ϵ values, specifically $\epsilon = 0.005$.

**FIGURE 7.** Domain for the WPT system.

Lastly, the effect of population size N is tested, and the results are listed in Table 3. The best results are obtained for a population \mathcal{P} of 20 individuals. It is important to note that these are the results of a specific test, however, some rules can be extracted for the selection of the user-defined parameters:

- 1) It is not convenient to use large or small, static, values of β . A scheme that adjusts β during algorithm iterations is preferable.
- 2) It is convenient to use a small value of ϵ .
- 3) Small populations do not perform well, as in many EAs. This is, however, not a drawback since even large populations can be evaluated in parallel.

C. DESIGN OF WIRELESS POWER TRANSFER DEVICE

In this example, the performance of GPBTO is tested against an in-house multi-objective Differential Evolution (DE) algorithm [66], for the design of a Wireless Power Transfer (WPT) device illustrated in Fig. 7. Exploiting the symmetries

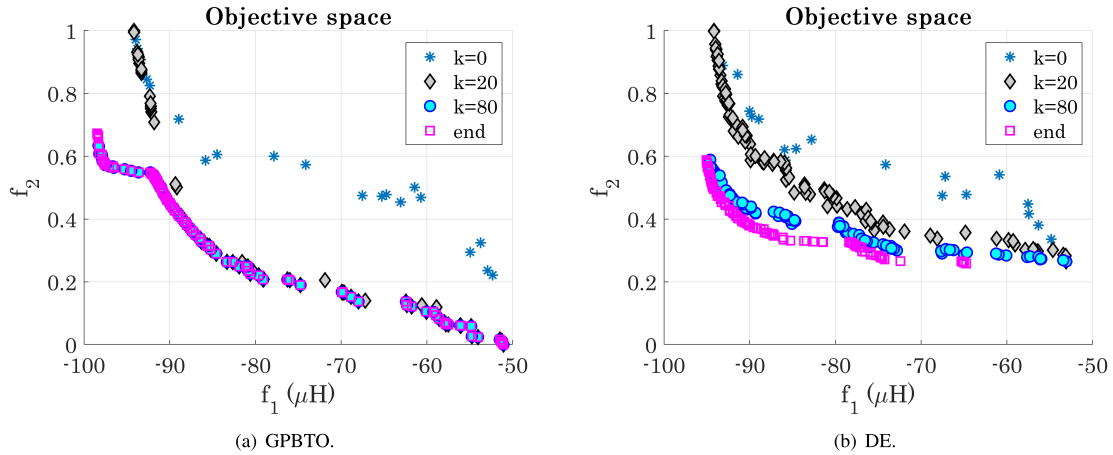


FIGURE 8. Objective space during algorithm iterations.

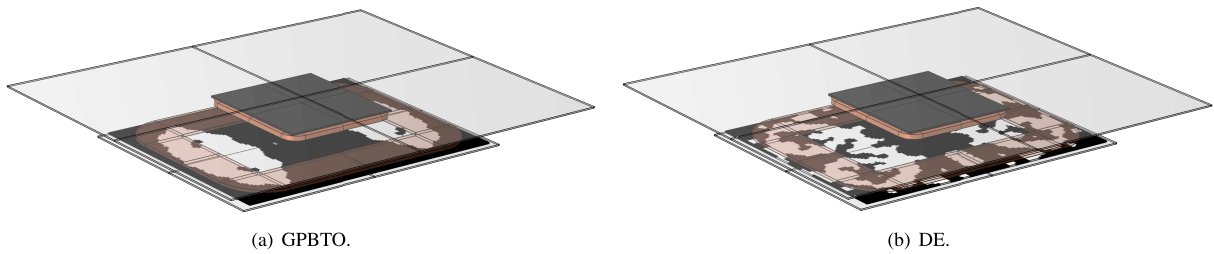


FIGURE 9. Final topology corresponding to the minimum value of f_1 .

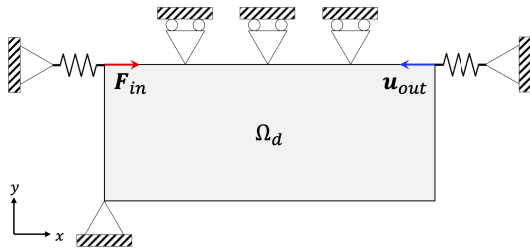


FIGURE 10. Domain and boundary conditions for the compliant mechanism.

of the problem, only a quarter of the domain is subsequently analyzed. The TO process in this test case, retrieved from [3], aims at finding the distribution of the relative permeability μ_r in Ω_d , corresponding to the lower ferrite plate, considering the two objectives:

$$\begin{aligned} f_1 &= -M(\mathbf{x}) \\ f_2 &= V(\mathbf{x})/V_{\Omega_d}, \end{aligned} \quad (22)$$

where M is the mutual inductance computed from the solution of a magnetostatic problem. According to (9), in this case, $\mathcal{M}_{void} = \mu_{r,void} = 1$ corresponds to air, while $\mathcal{M}_{fill} = \mu_{r,fill} = 3330$ corresponds to ferrite material. The number of decision variables, $b = 2640$, corresponds to the hexahedral elements discretizing Ω_d . For DE, a population of $N = 20$ individuals is selected for both approaches. Additionally, the mutation F and crossover CR parameters used in the DE are fixed at $F = 0.8$ and $CR = 0.5$. The maximum number

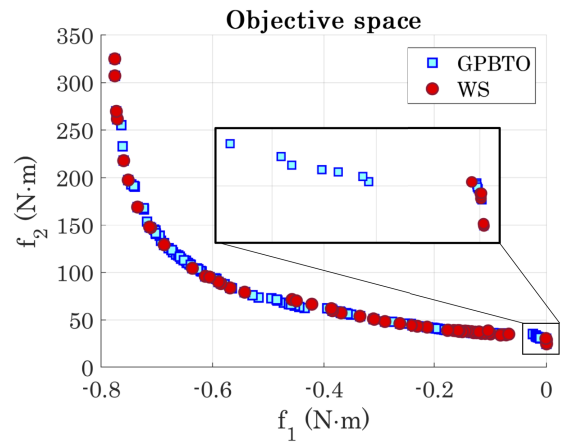


FIGURE 11. PF of CBOP TO problem for the compliant mechanism.

of iterations is set to $k_{max} = 250$, and both algorithms start with a randomly initialized population \mathcal{P}_0 . The points (f_1, f_2) stored in the archives \mathcal{F}_1 and \mathcal{F}_2 throughout the algorithm iterations are illustrated in Fig. 8. Both approaches are capable of evolving the population toward a Pareto-optimal solution; however, GPBTO explores a larger portion of the front with lower f_1 , which remains nondominated by other solutions. This suggests that DE requires more iterations and correction techniques to effectively guide population evolution. Notably, the total number of objective function evaluations remains the same for both methods.

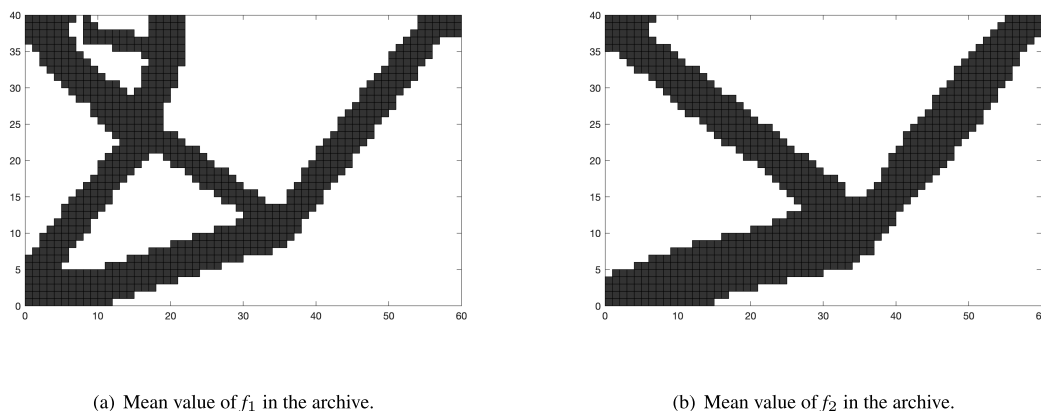


FIGURE 12. Topologies of compliant mechanism after optimization.

Moreover, it is recognized that DE, if not properly corrected, exhibits disconnected topologies if compared to the gradient-based approach [3], [67]. This can be seen in Fig. 9, where the topologies of Ω_d corresponding to the minimum value for f_1 at the end of algorithm iterations are illustrated.

D. DESIGN OF A COMPLIANT MECHANISM

In this experiment, a compliant mechanism through TO is designed. This test case has been chosen since it is a classical structural mechanics benchmark involving two conflicting objective functions [21]. The domain and boundary conditions for the mechanism are illustrated in Fig. 10. The optimization aims at maximizing flexibility while at the same time minimizing compliance, thus, maximizing the rigidity of the structure. Following the FEA approach described in Section IV-B, the two objectives are written as:

$$\begin{aligned} f_1(\mathbf{x}) &= -\mathbf{u}(\mathbf{x})^\top \Phi \\ f_2(\mathbf{x}) &= \mathbf{u}^\top(\mathbf{x})\mathbf{K}(\mathbf{x})\mathbf{u}(\mathbf{x}) \end{aligned} \quad (23)$$

where f_1 represents the mutual potential energy (MPE) and f_2 is the SE. The latter f_2 follows directly from the structural analysis excited by the external load \mathbf{F}_{in} , while f_1 follows from the application of a dummy load Φ at the output location, as explained in detail in [68] and [69]. The CBOP is completed by adding a volumetric constraint on the final amount of material with $E = E_{fill}$ in Ω_d , as defined in (10), with $\bar{V} = 0.3$.

In this example, a uniform grid consisting of $n_x = 60$ elements along x -coordinate and $n_y = 40$ elements along y -coordinate, for a total of $n_x n_y = 2400$ finite elements is used to discretize Ω_d , i.e. $n = 2400$ decision variables are used in this benchmark problem. The parameters of the GPBTO algorithm are tuned based on the results obtained in Section IV-B. In particular $\epsilon = 0.005$, β decreased with law (16), $N = 40$, and $k_{max} = 1000$. The computed PF is illustrated in Fig. 11. The PF obtained with the GPBTO algorithm and the WS method are reported. The latter is computed since the WS is recognized as the state-of-art for solving multi-objective TO problems, however, it can be noticed that the WS is not able to capture the correct trend of the PF in the bottom right

part. Indeed, in this region of the objective space, there is a convexity change, where the Pareto is irregular [70].

The topologies of the compliant mechanism corresponding to the mean value of f_1 and the mean of f_2 in \mathcal{A} are shown in Fig. 12.

V. CONCLUSION

This article introduces the concept of Pareto-optimal solutions within the gradient-based topology optimization (TO) framework based on binary decision variables, addressing conflicting objectives subject to constraints. The proposed GPBTO algorithm is specifically designed for bi-objective problems with a single constraint, a common scenario in engineering. Its performance is evaluated against standard methods, including the Weighted Sum (WS) approach and the stochastic Differential Evolution (DE) algorithm, using multi-objective problems from electrical and structural engineering applications. The experimental results showed that:

- 1) For convex Pareto fronts (PFs) the proposed algorithm matches the PF obtained via the WS method, demonstrating the validity of the approach.
- 2) Thanks to gradient-based evolution, GPBTO constructs topologies with improved element connectivity compared to the stochastic DE.
- 3) Non-convex parts of the PF can be obtained with the proposed approach as shown in the numerical experiments, demonstrating the main merit of the algorithm.

Future activities will be devoted to the extension of the proposed GPBTO to many-objective functions and multiple constraints and the application to a larger class of engineering problems.

REFERENCES

- [1] O. Sigmund, "On the design of compliant mechanisms using topology optimization," *J. Struct. Mech.*, vol. 25, no. 4, pp. 493–524, Jan. 1997.
- [2] A. S. D. C. Azevêdo, S. Ranjbarzadeh, R. D. S. Gioria, E. C. N. Silva, and R. Picelli, "On the multi-objective perspective of discrete topology optimization in fluid-structure interaction problems," *Appl. Math. Model.*, vol. 127, pp. 1–17, Mar. 2024.

- [3] F. Lucchini, R. Torchio, V. Cirimele, P. Alotto, and P. Bettini, "Topology optimization for electromagnetics: A survey," *IEEE Access*, vol. 10, pp. 98593–98611, 2022.
- [4] H. Igarashi, *Topology Optimization and AI-Based Design of Power Electronic and Electrical Devices: Principles and Methods*. Hoboken, NJ, USA: Wiley, 2024.
- [5] C.-H. Im, H.-K. Jung, and Y.-J. Kim, "Hybrid genetic algorithm for electromagnetic topology optimization," *IEEE Trans. Magn.*, vol. 39, no. 5, pp. 2163–2169, Sep. 2003.
- [6] O. Sigmund and K. Maute, "Topology optimization approaches: A comparative review," *Struct. Multidisciplinary Optim.*, vol. 48, no. 6, pp. 1031–1055, Dec. 2013.
- [7] D. Guirguis, N. Aulig, R. Picelli, B. Zhu, Y. Zhou, W. Vicente, F. Iorio, M. Olhofer, W. Matusik, C. A. Coello Coello, and K. Saitou, "Evolutionary black-box topology optimization: Challenges and promises," *IEEE Trans. Evol. Comput.*, vol. 24, no. 4, pp. 613–633, Aug. 2020.
- [8] I. Sosnovik and I. Oseledets, "Neural networks for topology optimization," *Russian J. Numer. Anal. Math. Model.*, vol. 34, no. 4, pp. 215–223, Aug. 2019.
- [9] R. V. Woldseth, N. Aage, J. A. Bærentzen, and O. Sigmund, "On the use of artificial neural networks in topology optimisation," *Struct. Multidisciplinary Optim.*, vol. 65, no. 10, p. 294, Oct. 2022.
- [10] O. Sigmund, "On the usefulness of non-gradient approaches in topology optimization," *Struct. Multidisciplinary Optim.*, vol. 43, no. 5, pp. 589–596, May 2011.
- [11] K. Deb, A. Pratap, S. Agarwal, and T. Meyarivan, "A fast and elitist multiobjective genetic algorithm: NSGA-II," *IEEE Trans. Evol. Comput.*, vol. 6, no. 2, pp. 182–197, Apr. 2002.
- [12] E. Biyikli and A. C. To, "Proportional topology optimization: A new non-sensitivity method for solving stress constrained and minimum compliance problems and its implementation in MATLAB," *PLoS ONE*, vol. 10, no. 12, Dec. 2015, Art. no. e0145041.
- [13] L. Dos Santos Coelho and P. Alotto, "Multiobjective electromagnetic optimization based on a nondominated sorting genetic approach with a chaotic crossover operator," *IEEE Trans. Magn.*, vol. 44, no. 6, pp. 1078–1081, Jun. 2008.
- [14] R. Bosshard and J. W. Kolar, "Multi-objective optimization of 50 kW/85 kHz IPT system for public transport," *IEEE J. Emerg. Sel. Topics Power Electron.*, vol. 4, no. 4, pp. 1370–1382, Dec. 2016.
- [15] J. Wang, X. Liu, and U. Desideri, "Performance improvement evaluation of latent heat energy storage units using improved bi-objective topology optimization method," *Appl. Energy*, vol. 364, Jun. 2024, Art. no. 123131.
- [16] H.-Z. Zhang, P. Luo, and X.-X. Yuan, "Reinforcement layout design for deep beams based on bi-objective topology optimization," *Autom. Construction*, vol. 158, Feb. 2024, Art. no. 105237.
- [17] D. Guirguis and M. F. Aly, "An evolutionary multi-objective topology optimization framework for welded structures," in *Proc. IEEE Congr. Evol. Comput. (CEC)*, Jul. 2016, pp. 372–378.
- [18] N. Aulig and M. Olhofer, "Evolutionary computation for topology optimization of mechanical structures: An overview of representations," in *Proc. IEEE Congr. Evol. Comput. (CEC)*, Jul. 2016, pp. 1948–1955.
- [19] S. Doi, H. Sasaki, and H. Igarashi, "Multi-objective topology optimization of rotating machines using deep learning," *IEEE Trans. Magn.*, vol. 55, no. 6, pp. 1–5, Jun. 2019.
- [20] Y. Li, L. Liu, S. Yang, Z. Ren, and Y. Ma, "A multi-objective topology optimization methodology and its application to electromagnetic actuator designs," *IEEE Trans. Magn.*, vol. 56, no. 2, pp. 1–4, Feb. 2020.
- [21] Z. Luo, L. Chen, J. Yang, Y. Zhang, and K. Abdel-Malek, "Compliant mechanism design using multi-objective topology optimization scheme of continuum structures," *Struct. Multidisciplinary Optim.*, vol. 30, no. 2, pp. 142–154, Aug. 2005.
- [22] K. Izui, T. Yamada, S. Nishiwaki, and K. Tanaka, "Multiobjective optimization using an aggregative gradient-based method," *Struct. Multidisciplinary Optim.*, vol. 51, no. 1, pp. 173–182, Jan. 2015.
- [23] J. Wang, D. Melideo, X. Liu, and U. Desideri, "Comparative study on topology optimization of microchannel heat sink by using different multi-objective algorithms and objective functions," *Appl. Thermal Eng.*, vol. 252, Sep. 2024, Art. no. 123606.
- [24] C. Ma, J. Hu, M. Li, X. Deng, J. Yang, J. He, C. Hua, L. Wang, J. Liu, K. Liu, Y. Zhou, M. Li, J. Zhou, X. Deng, and S. Weng, "Multi-objective topology optimization for cooling element of precision gear grinding machine tool," *Int. Commun. Heat Mass Transf.*, vol. 160, Nov. 2024, Art. no. 108356.
- [25] M. Hu and U. K. Madawala, "Magnetic structure design in IPT systems based on topology optimization," *IEEE Trans. Transport. Electrific.*, vol. 11, no. 2, pp. 5374–5386, Apr. 2025.
- [26] R. T. Marler and J. S. Arora, "The weighted sum method for multi-objective optimization: New insights," *Struct. Multidisciplinary Optim.*, vol. 41, no. 6, pp. 853–862, Jun. 2010.
- [27] I. Y. Kim and O. L. de Weck, "Adaptive weighted-sum method for bi-objective optimization: Pareto front generation," *Struct. Multidisciplinary Optim.*, vol. 29, no. 2, pp. 149–158, Feb. 2005.
- [28] T. Cherière, "Towards topology optimization of a hybrid-excited machine using recursive material interpolation," 2024, *arXiv:2404.18625*.
- [29] N. Ryu, M. Seo, and S. Min, "Multi-objective topology optimization incorporating an adaptive weighed-sum method and a configuration-based clustering scheme," *Comput. Methods Appl. Mech. Eng.*, vol. 385, Nov. 2021, Art. no. 114015.
- [30] D. Chen, P. Kumar, Y. Kametani, and Y. Hasegawa, "Multi-objective topology optimization of heat transfer surface using level-set method and adaptive mesh refinement in OpenFOAM," *Int. J. Heat Mass Transf.*, vol. 221, Apr. 2024, Art. no. 125099.
- [31] J. Wang, U. Desideri, and X. Liu, "Multi-objective structure optimization and performance analysis of catalytic micro-reactor channel designed by an improved topology optimization model," *Appl. Thermal Eng.*, vol. 244, May 2024, Art. no. 122742.
- [32] J. Fliege and B. F. Svaiter, "Steepest descent methods for multicriteria optimization," *Math. Methods Oper. Res.*, vol. 51, no. 3, pp. 479–494, Aug. 2000.
- [33] P. Gangl, S. Köthe, C. Mellak, A. Cesarano, and A. Mütze, "Multi-objective free-form shape optimization of a synchronous reluctance machine," *COMPEL-Int. J. Comput. Math. Electr. Electron. Eng.*, vol. 41, no. 5, pp. 1849–1864, Aug. 2022.
- [34] A. Cesarano and P. Gangl, "Tracing Pareto-optimal points for multi-objective shape optimization applied to electric machines," 2024, *arXiv:2404.12205*.
- [35] N. Pholdee and S. Bureerat, "Performance enhancement of multiobjective evolutionary optimisers for truss design using an approximate gradient," *Comput. Struct.*, vols. 106–107, pp. 115–124, Sep. 2012.
- [36] M. Bujny, N. Aulig, M. Olhofer, and F. Duddeck, "Hybrid evolutionary approach for level set topology optimization," in *Proc. IEEE Congr. Evol. Comput. (CEC)*, Jul. 2016, pp. 5092–5099.
- [37] Y. Tian, H. Chen, H. Ma, X. Zhang, K. C. Tan, and Y. Jin, "Integrating conjugate gradients into evolutionary algorithms for large-scale continuous multi-objective optimization," *IEEE/CAA J. Autom. Sinica*, vol. 9, no. 10, pp. 1801–1817, Oct. 2022.
- [38] J. D. Deaton and R. V. Grandhi, "A survey of structural and multidisciplinary continuum topology optimization: Post 2000," *Struct. Multidisciplinary Optim.*, vol. 49, no. 1, pp. 1–38, Jan. 2014.
- [39] F. Wang, B. S. Lazarov, and O. Sigmund, "On projection methods, convergence and robust formulations in topology optimization," *Struct. Multidisciplinary Optim.*, vol. 43, no. 6, pp. 767–784, Dec. 2010.
- [40] C.-Y. Wu and K.-Y. Tseng, "Topology optimization of structures using modified binary differential evolution," *Struct. Multidisciplinary Optim.*, vol. 42, no. 6, pp. 939–953, Dec. 2010.
- [41] G.-C. Luh, C.-Y. Lin, and Y.-S. Lin, "A binary particle swarm optimization for continuum structural topology optimization," *Appl. Soft Comput.*, vol. 11, no. 2, pp. 2833–2844, Mar. 2011.
- [42] R. Sivapuram and R. Picelli, "Topology optimization of binary structures using integer linear programming," *Finite Elements Anal. Design*, vol. 139, pp. 49–61, Nov. 2017.
- [43] L. M. Antonio and C. A. C. Coello, "Use of cooperative coevolution for solving large scale multiobjective optimization problems," in *Proc. IEEE Congr. Evol. Comput.*, Jun. 2013, pp. 2758–2765.
- [44] S. Mukherjee, D. Lu, B. Raghavan, P. Breitkopf, S. Dutta, M. Xiao, and W. Zhang, "Accelerating large-scale topology optimization: State-of-the-art and challenges," *Arch. Comput. Methods Eng.*, vol. 28, no. 7, pp. 4549–4571, Dec. 2021.
- [45] Y. Tian, Y. Feng, X. Zhang, and C. Sun, "A fast clustering based evolutionary algorithm for super-large-scale sparse multi-objective optimization," *IEEE/CAA J. Autom. Sinica*, vol. 10, no. 4, pp. 1048–1063, Apr. 2023.
- [46] M. Zhou, M. Cui, D. Xu, S. Zhu, Z. Zhao, and A. Abusorrah, "Evolutionary optimization methods for high-dimensional expensive problems: A survey," *IEEE/CAA J. Autom. Sinica*, vol. 11, no. 5, pp. 1092–1105, May 2024.

- [47] S. Sanogo and F. Messine, "Topology optimization in electromagnetism using SIMP method: Issues of material interpolation schemes," *COMPEL-Int. J. Comput. Math. Electr. Electron. Eng.*, vol. 37, no. 6, pp. 2138–2157, Nov. 2018.
- [48] R. El Bechari, F. Guyomarch, and S. Brisset, "The adjoint variable method for computational electromagnetics," *Mathematics*, vol. 10, no. 6, p. 885, Mar. 2022.
- [49] A. Chandrasekhar, S. Sridhara, and K. Suresh, "AuTO: A framework for automatic differentiation in topology optimization," *Struct. Multidisciplinary Optim.*, vol. 64, no. 6, pp. 4355–4365, Dec. 2021.
- [50] K. Svanberg and M. Werme, "Sequential integer programming methods for stress constrained topology optimization," *Struct. Multidisciplinary Optim.*, vol. 34, no. 4, pp. 277–299, May 2007.
- [51] R. Picelli, R. Sivapuram, and Y. M. Xie, "A 101-line MATLAB code for topology optimization using binary variables and integer programming," *Struct. Multidisciplinary Optim.*, vol. 63, no. 2, pp. 935–954, Feb. 2021.
- [52] R. E. Bechari, V. Martin, F. Gillon, F. Guyomarch, S. Brisset, D. Najjar, and J.-F. Witz, "From topology optimization to 3-D printing of an electromagnetic core," *IEEE Trans. Magn.*, vol. 59, no. 5, pp. 1–4, May 2023.
- [53] F. Lucchini, R. Torchio, P. Bettini, and F. Dughiero, "TopIE: An integral equation tool for topology optimization in electromagnetics," *IEEE Trans. Antennas Propag.*, vol. 72, no. 1, pp. 683–692, Jan. 2024.
- [54] J. L. Gearhart, K. L. Adair, J. D. Durfee, K. A. Jones, N. Martin, and R. J. Detry, "Comparison of open-source linear programming solvers," Sandia Nat. Lab. (SNL-NM), Albuquerque, NM, USA, Tech. Rep. SAND2013-8847, 2013.
- [55] O. Sigmund and J. Petersson, "Numerical instabilities in topology optimization: A survey on procedures dealing with checkerboards, mesh-dependencies and local minima," *Struct. Optim.*, vol. 16, no. 1, pp. 68–75, Aug. 1998.
- [56] J. Seok Choi and J. Yoo, "Structural topology optimization of magnetic actuators using genetic algorithms and ON/OFF sensitivity," *IEEE Trans. Magn.*, vol. 45, no. 5, pp. 2276–2279, May 2009.
- [57] C. A. C. Coello, *Evolutionary Algorithms for Solving Multi-Objective Problems*. Cham, Switzerland: Springer, 2007.
- [58] Y. G. Woldesenbet, G. G. Yen, and B. G. Tessema, "Constraint handling in multiobjective evolutionary optimization," *IEEE Trans. Evol. Comput.*, vol. 13, no. 3, pp. 514–525, Jun. 2009.
- [59] R. Mallipeddi and P. N. Suganthan, "Ensemble of constraint handling techniques," *IEEE Trans. Evol. Comput.*, vol. 14, no. 4, pp. 561–579, Aug. 2010.
- [60] K. Deb, "An efficient constraint handling method for genetic algorithms," *Comput. Methods Appl. Mech. Eng.*, vol. 186, nos. 2–4, pp. 311–338, Jun. 2000.
- [61] S. S. Dey, Y. Dubey, and M. Molinaro, "Branch-and-Bound solves random binary IPs in polytime," in *Proc. ACM-SIAM Symp. Discrete Algorithms (SODA)*, Jan. 2021, pp. 579–591.
- [62] A. Zhou, Y. Jin, Q. Zhang, B. Sendhoff, and E. Tsang, "Combining model-based and genetics-based offspring generation for multi-objective optimization using a convergence criterion," in *Proc. IEEE Int. Conf. Evol. Comput.*, May 2006, pp. 892–899.
- [63] H. Ishibuchi, H. Masuda, Y. Tanigaki, and Y. Nojima, "Modified distance calculation in generational distance and inverted generational distance," in *Proc. 8th Int. Conf. Evol. Multi-Criterion Optim.*, vol. 9019, Guimarães, Portugal. Cham, Switzerland: Springer, Jan. 2015, pp. 110–125.
- [64] M. P. Bendsoe and O. Sigmund, *Topology Optimization: Theory, Methods, and Applications*. Cham, Switzerland: Springer, 2013.
- [65] Y. Shi and R. Eberhart, "A modified particle swarm optimizer," in *Proc. IEEE Int. Conf. Evol. Comput. IEEE World Congr. Comput. Intell.*, Jun. 1998, pp. 69–73.
- [66] P. Alotto, "A hybrid multiobjective differential evolution method for electromagnetic device optimization," *COMPEL-Int. J. Comput. Math. Electr. Electron. Eng.*, vol. 30, no. 6, pp. 1815–1828, Nov. 2011.
- [67] Y. Otomo and H. Igarashi, "A 3-D topology optimization of magnetic cores for wireless power transfer device," *IEEE Trans. Magn.*, vol. 55, no. 6, pp. 1–5, Jun. 2019.
- [68] E. Lee and H. C. Gea, "A strain based topology optimization method for compliant mechanism design," *Struct. Multidisciplinary Optim.*, vol. 49, no. 2, pp. 199–207, Feb. 2014.
- [69] M. N. Nguyen, M. T. Tran, H. Q. Nguyen, and T. Q. Bui, "A multi-material proportional topology optimization approach for compliant mechanism problems," *Eur. J. Mechanics-A/Solids*, vol. 100, Mar. 2023, Art. no. 104957.
- [70] Y. Hua, Q. Liu, K. Hao, and Y. Jin, "A survey of evolutionary algorithms for multi-objective optimization problems with irregular Pareto fronts," *IEEE/CAA J. Autom. Sinica*, vol. 8, no. 2, pp. 303–318, Feb. 2021.



FRANCESCO LUCCHINI received the M.S. degree in mathematical engineering from the University of Padova, Padua, Italy, in 2019, and the dual Ph.D. degree in fusion science and engineering from the University of Padova and Ghent University, Ghent, Belgium, in 2023.

He is currently an Assistant Professor (RTDa) with the University of Padova. His research interests include numerical methods, optimizations, and the development of integral formulations for the study

of electromagnetic devices.



RICCARDO TORCHIO (Member, IEEE) was born in Padua, Italy, in 1992. He received the M.S. degree in electrical engineering from the University of Padova, Padua, in 2016, and the dual Ph.D. degree in electrical engineering from the University of Padova and Grenoble Electrical Engineering Laboratory (G2ELab), Université Grenoble Alpes, France, in December 2019.

He is currently with the University of Padova, as an Assistant Professor (RTDb). His research

interests include numerical methods, optimizations, low-rank compression techniques, uncertainty quantifications, wireless power transfer applications, model order reduction, model predictive control, and the development of integral formulations for the study of low- and high-frequency electromagnetic devices.



PIERGIORGIO ALOTTO was born in Genoa, Italy, in 1968. He received the degree and Ph.D. degrees (Hons.) in electrical engineering from the University of Genoa, in 1992 and 1997, respectively.

From 1992 to 1994, he was a Software Development Engineer with Vector Fields Ltd., Oxford, U.K., a scientific software house. From 1997 to 2005, he was an Assistant Professor with the University of Genoa. He joined the

University of Padua, Italy, in 2005, where he has been a Full Professor of electrical engineering, since 2018. His scientific interests, which have led to over 150 indexed publications in peer-reviewed international journals and conference proceedings, include several aspects of the computation of electromagnetic fields and the design of electromagnetic devices. He is an inventor of three national patents (one with PCT extension) concerning an electrostatic purification filter, a magnetic differential gear, and a battery-operated system for the logging industry.

...